HHS Public Access

Author manuscript

Nanomedicine. Author manuscript; available in PMC 2017 April 01.

Published in final edited form as:

Nanomedicine. 2016 April ; 12(3): 589–600. doi:10.1016/j.nano.2015.11.010.

EGFR-Targeted Gelatin Nanoparticles for Systemic Administration of Gemcitabine in an Orthotopic Pancreatic Cancer Model

Amit Singh, **Jing Xu**, **George Mattheolabakis**, and **Mansoor Amiji***

Department of Pharmaceutical Sciences, School of Pharmacy, Northeastern University, Boston, MA 02115

Abstract

In this study, we have formulated redox-responsive epidermal growth factor receptor (EGFR)-targeted type B gelatin nanoparticles as a targeted vector for systemic delivery of gemcitabine therapy in pancreatic cancer. The gelatin nanoparticles were formed by ethanol-induced desolvation process to encapsulate the bound drug. The surface of the nanoparticles was decorated either with poly(ethylene glycol) (PEG) chains to impart enhanced circulation time and with EGFR targeting peptide to confer target specificity. Our *in vitro* studies in Panc-1 human pancreatic ductal adenocarcinoma cells confirm that gemcitabine encapsulated in EGFR-targeted gelatin nanoparticles, released through disulfide bond cleavage, had a significantly improved cytotoxic profile. Further, the *in vivo* anticancer activity was evaluated in an orthotopic pancreatic adenocarcinoma tumor bearing SCID beige mice, which confirmed that EGFR-targeted gelatin nanoparticles could efficiently deliver gemcitabine to the tumor leading to higher therapeutic benefit as compared to the drug in solution.

Keywords

Thiolated gelatin nanoparticles; Gemcitabine; Orthotopic tumor model; Panc-1, Pancreatic ductal adenocarcinoma (PDAC); epidermal growth factor receptor (EGFR) targeting

BACKGROUND

Pancreatic cancer is among the leading causes of cancer-related deaths with an extremely poor prognosis and a dismal five-year survival rate of less than 5% (1–3). Among the patients detected with pancreatic cancer, only 10% present a surgically resectable disease, where the tumor mass can be excised by surgical intervention followed by preventive chemo and/or radiation therapy. However, in majority of pancreatic cancer cases, the post-surgery relapse of the disease leads to a highly aggressive and metastatic form that does not respond

Corresponding author: Tel. (617) 373-3137, Fax (617) 373-8886, m.amiji@neu.edu.

Conflict of Interests: The authors declare no conflicts of interest.

to any therapy. Patients suffering from advanced stage local tumor have a slightly longer median survival of 6–10 months, but those reported with metastatic stage of the disease have a mere 3–6 months of median survival rate (4–8). Chemotherapy remains the only option for treatment of metastatic pancreatic cancer even though the approach tends to be mostly palliative with no major survival advantage (4). Pancreatic cancer possesses a highly complex genetic, physical, and physiological makeup of the tumor microenvironment and the presence of abundant stromal components along with the neoplastic cells leads to poor vascularization that severely limits drug perfusion into the tumor upon systemic administration (9). As such, there is an urgent need for more effective therapeutic approach focusing on targeted delivery to overcome the formidable challenges posed by pancreatic cancer.

Gemcitabine (GEMZAR®), an antimetabolite anticancer agent, has been the drug for standard care against pancreatic cancer since 1997, when it was first approved as the front line agent for chemotherapy. However, there has been considerable debate on the success of gemcitabine as single therapeutic agent in improving the survival benefit in patients suffering from advanced local and metastatic pancreatic cancer (10). In majority of these studies, the prognostic effect of gemcitabine therapy is modest and incremental at best. The poor clinical outcome from gemcitabine could be attributed to its poor residence time in the body, unfavorable pharmacokinetic and pharmacodynamic (PK/PD) profile, and the complex tumor microenvironment resulting in minimal penetration of the drug in the tumor cells (11). Although there has been a recent surge in preclinical and clinical studies with combination cytotoxic and molecularly targeted therapeutics in pancreatic cancer, the therapeutic benefit in terms of improved clinical outcomes has not been realized so far (1, 12). After several failed clinical trials, FOLFIRINOX therapy (bolus plus infusional fluorouracil, leucovorin, irinotecan and oxaliplatin) was replaced as the new standard of care, first line treatment of pancreatic cancer due to an improved median survival rate of approximately 11 months (13). Recent clinical studies have shown marked improvements in the treatment of pancreatic cancer when gemcitabine is combined with albumin-bound paclitaxel nanoparticles (Abraxane®) (14).

Previous work from our group has reported on the use of type B gelatin-based non-condensing, stimuli-responsive nanoparticle system for delivery of nucleic acids *in vitro* as well as *in vivo* in many different tumor models (15–22). Type B gelatin with an isoelectric point of 4–5, is a natural biocompatible, non-immunogenic, and biodegradable polymer, which is considered by the U.S. Food and Drug Administration as a "*generally regarded as safe*" *(GRAS)* material that has been extensively used in food industry. The biopolymeric nature of gelatin also presents a large number of functional groups, such as carboxyl and amine groups, that can be used for chemical manipulation of the backbone to impart desired properties to the polymer. Thiol modification of gelatin leads to formation of redox-responsive disulfide bridges when the nanoparticle is formed by the desolvation process (15, 16). Under the highly reducing environment found inside the cancer cells, the disulfide bridges are cleaved in response to higher intracellular concentrations of glutathione resulting in the release of the nucleic acid payload (15, 19). *In vitro* assessment of the EGFR-targeted nanoparticles loaded with wt-p53 plasmid confirmed a successful receptor-mediated

delivery and subsequent expression of wt-p53 protein leading to induction of apoptosis in Panc-1 cells (20). Biodistribution and pharmacokinetic studies in Panc-1 subcutaneous xenograft tumor bearing SCID beige mice further revealed that the EGFR targeted nanoparticles could preferentially accumulate in the tumor mass and efficacy studies corroborated with this observation since targeted nanoparticles show an improved inhibition in tumor growth compared to non-targeted nanoparticles (22). We have further demonstrated that gelatin nanoparticles could also be used for delivery of gemcitabine via disulfide chemical conjugation on the polymer backbone and thus prove to be an exciting delivery system for a combination treatment of pancreatic cancer.

Lack of a suitable preclinical cancer model is one of the leading causes of failure of promising drug candidates at the clinical stage. Majority of literature on treatment of pancreatic cancer have used subcutaneous xenograft models that do not accurately recapitulate the physical and biological nuances of the actual disease. However, this model has been extensively used due to the ease of development and low associated cost, while compromising on clinical suitability. More recently, genetically engineered mouse models (GEMM) with specific mutations relevant to the disease (23) and patient-derived heterotropic xenograft models with actual mutations (24) manifested by the patients, have been considered as more clinically relevant models, but suffer from high developmental cost. Surgical orthotopic model for pancreatic cancer is another suitable alternative, where the human cancer cells are surgically implanted in the pancreas to provide an ideal microenvironment for tumor growth and metastasis (25). This animal model presents an ideal system for drug screening studies *in vivo* due to its higher similarity to an actual clinical presentation. In this study, we have developed multifunctional nanoparticles composed of thiolated gelatin that possess long circulating and redox-responsive properties as well as specific targeting to the EGFR receptor for delivery of gemcitabine *in vitro* and *in vivo*. *In vitro* characterization of the activity confirmed that nanoparticle-based systems outperformed the drug in solution and their *in vivo* anticancer activity was further confirmed in orthotopic Panc-1 human pancreatic adenocarcinoma tumor bearing SCID beige mice.

METHODS

Materials

Reagent grade succinimidyl 3-[2-pyridyldithio]-propionate) (SPDP), (3-(4,5-dimethylthiazol-2-yl)-2,5-diphenyltetrazolium bromide) (MTT reagent), 2-iminothiolane hydrochloride, bovine type B gelatin, glutathione (GSH), dithiothreitol (DTT), Triton™ X-114, and protease were all purchased from Sigma Aldrich (St. Louis, MO, USA) and were used without further purification. Gemcitabine (2’-deoxy-2’2’-diflurocytidine) free base was purchased from Carbosynth (Berkshire, UK). The functional PEG derivatives, methoxy-PEGsuccinimidylcarbosyl methyl ester (mPEG-SCM, MW 2,000 Da) and maleimide-PEG-SCM (MAL-PEG-SCM, MW 2,000 Da), were purchased from Creative PEGWorks (Winston Salem, NC, USA).

Cell Lines

Human pancreatic ductal adenocarcinoma cells Panc-1 were acquired from ATCC (Manassas, VA) while luciferase-expressing Panc-1 cells (Panc-1 luc) were kindly provided by Prof. Dawn E. Quelle from University of Iowa (Iowa City, IO). Both the cell lines were subcultured in Dulbecco's Modified Eagle Medium (DMEM) supplemented with 10 % fetal bovine serum (FBS) and 1 % Pen-Strep.

Synthesis of Thiolated Gelatin (SH-Gel)

Thiolated gelatin was synthesized according to our previously optimized and established protocol reported elsewhere (16, 22) and briefly described as supporting information (SI. 2).

Synthesis of Gemcitabine-SPDP (Gem-SPDP) Conjugate

Gem-SPDP was first synthesized by a chemical conjugation scheme shown in Figure 1. Briefly, 10 mg base form of gemcitabine was dissolved in 5 mL dry methanol (100%) and reacted with 100 mg SPDP under dark conditions with continuous stirring at 80 °C under reflux conditions for 48 h. The final product of the reaction was monitored by thin-layer chromatography (TLC) [*Rf* 0.67 (CHCl3/MeOH, 8:2)] to confirm the conjugate formation. The conjugate was purified by normal phase flash chromatography (Interchim puriFlash 430evo, Montlucon, France) using first five column volumes of dichloromethane followed by 0–10 % Methanol/dichloromethane gradient. The identity of the conjugate in the elute fractions was confirmed by TLC and the fractions containing the conjugate were initially dried under vacuum using rotary evaporator IKA RV10 at 60 °C and further incubated in vacuum desiccator overnight to remove any residual solvent. The purified conjugate was stored at −20 °C until further use.

Gemcitabine-SPDP Conjugation with Thiolated Gelatin

For conjugation with gemcitabine-SPDP, thiolated gelatin was dissolved into 0.1 M PBS/EDTA (100 mM sodium phosphate, 150 mM NaCl, 1 mM EDTA, 0.02% sodium azide, pH 7.5) at concentration of 10 mg/mL. Gem-SPDP conjugate dissolved in 1 mL DMSO was added to thiolated gelatin solution and stirred overnight at room temperature to allow the disulfide conjugation. The disulfide conjugate gemcitabine-gelatin (Gem-Gel) thus formed was dialyzed against deionized water overnight, freeze dried and the purified polymers were used for drug-encapsulating nanoparticles synthesis.

Nanoparticle Formulation and Characterization

Gelatin nanoparticles encapsulating gemcitabine were prepared by desolvation process that has been developed and optimized in our lab (15, 16, 22) and described as supporting information (SI. 3). The average hydrodynamic diameter and the polydispersity index (PDI) of the nanoparticles were measured by dynamic light scattering at room temperature and a 90° fixed angle using Zetasizer ZS (Malvern, Worcestershire, UK). Similarly, the zeta potential of the nanoparticles was measured using an electrophoretic cell. Finally, the morphology of the nanoparticles was observed under transmission electron microscope. The nanoparticles were drop coated on a formvar carboncoated copper grid (Electron Microscopy Science, Hatfield, PA) and were allowed to stand for 2 min, following which;

the excess fluid was drained using Whatman filter paper. The sample was further negatively stained using 1.5% uranyl acetate for 30 s at room temperature and excess stain was drained using Whatman filter paper and the grid was air-dried prior to imaging. The samples were imaged under a JEOL 100-X transmission electron microscope (Peobody, MA) using an acceleration voltage of 80 MeV.

Gemcitabine Loading Study by HPLC Assay

A high pressure liquid chromatography (HPLC) assay was developed for studying the retention properties of the SPDP, Gem and the Gem-SPDP conjugate itself and further use it to assess the drug loading efficiency within the nanoparticles. A Waters LC (model 2487, Waters Corporation, Milford) consisting of two pumps, autosampler and a UV detector was used for the analysis. Empower 3 software interfaced with the LC was used for instrument control, data acquisition and processing. A C_{18} column was used for analysis and the mobile phase consisted of 20% methanol/water (1:1) and 80% of 0.5 M ammonium acetate solution. The elution was performed using an isocratic flow rate of 1 ml/min and was observed at a wavelength of 268 nm. A standard curve was established with pure gemcitabine drug and all drug concentrations were calculated according to it. The Gem-Gel nanoparticles (10 mg/mL) were treated with 5 mM DTT and/or 0.2 mg/ml protease for 1 hour to degrade the gelatin nanoparticles and release the drug conjugate.

^{1}H-NMR and LC/MS Analysis of Gem-SPDP Conjugate

Proton nuclear magnetic resonance (^{1}H-NMR) spectroscopy was employed to characterize the Gem-SPDP conjugate in order to confirm the conjugation, as well as, the purity of the synthesized material. A sample (3 mg) of column-purified Gem-SPDP conjugate was dissolved in deuterated dimethylsulfoxide (DMSO) and was characterized using a 500 MHz ^{1}H-NMR spectrometer (Varian Inc., CA). For the liquid chromatography/mass spectrometry (LC/MS) analysis, a 1 mg/ml solution of the conjugate in methanol was further diluted 1000× with methanol and characterized on Agilent 1200 Infinity series LC coupled with 6120 quadrupole MS (Agilent Technologies, Santa Clara, CA, USA) operating in positive ion mode to obtain the mass spectra of the conjugate.

Western Blot Analysis of EGFR expression in Cells

Panc-1 and Panc-1 luc cells were analyzed by western blot to confirm EGFR expression. The detailed protocol of analysis has been provided as supporting information (SI. 5).

In Vitro Luciferase Activity Assay in Panc-1 luc Cells

The bioluminescence activity of the Panc-1 luc cells was confirmed by an *in vitro* activity assay. The detailed method has been provided in supporting information (SI. 6).

In Vitro Cytotoxicity Studies

In vitro cytotoxicity assessments were conducted for non-targeted and EGFR-targeted redox responsive Gem-Gel nanoparticles. Panc-1 cells were cultured overnight at a cell density of 5000 cells/well in a 96-well plate in 200 μl of supplemented DMEM media. Growth media was replaced with serum-supplemented media containing 0.1 nM–10 μM gemcitabine either

as free drug or encapsulated in nanoparticles. Poly(ethylene imine) (PEI, MW 10kDa), a known cytotoxic cationic polymer, was used as positive control for all cytotoxicity experiments. Cells were treated with gemcitabine or gemcitabine conjugated nanoparticles, SPDP alone or Gem-SPDP for 72 hours and replaced with 20 μL MTS reagent and 100μL culture media. After incubation for 3 hours at 37 °C in 5% CO_2 environment, the excess media was removed carefully without disturbing the cells and lysing the cells using 200 μl DMSO dissolved the formed formazan crystals. The absorption of the formazan product was measured at 490 nm with BioTek Synergy® HT plate reader (Winooski, VT). The relative viability of cells was expressed as the ratio of absorbance of drug treated cells relative to negative control and plotted as a function of gemcitabine concentration. GraphPad® PRISM software was used to analyze cytotoxicity data and calculate IC_{50} value for different formulations.

Development of an Orthotopic Surgical Pancreatic Adenocarcinoma Model

Orthotopic surgical model of Panc-1 luc ductal adenocarcinoma model was developed in nude and severe combined immunodeficiency (SCID) beige mice was developed to compare the timeline of tumor growth and metastasis (Supporting Information, SI. 7, 8). Tumor development and metastatic colonization were monitored by serial bioluminescence imaging on the IVIS system (Caliper Life Sciences (Hopkinton, MA)) at weekly intervals (26). The region of interest (ROI) was automatically detected by software and total luminescence counts were quantified using Living Image software v2.50 (Caliper Life Sciences, Hopkinton, MA). Animals were observed twice weekly for adverse events associated with tumor growth, at which time mice were euthanized. All animal handling and procedures were exercised according to protocol approved by Northeastern University's Institutional Animal Care and Use Committee (NU-IACUC) and the Biological Safety Committee within the Office of Environmental Health and Safety. The animals were housed in a group of 5 per cage and were supplied with sterile rodent pellets and water *ad libitum*.

Characterization of an Orthotopic Pancreatic Tumor Model

The blood collected from the tumor bearing mice were characterized for white blood cell count while organ and tumor tissues were studied by histopathological analysis. At established time points, blood samples were collected in EDTA coated K2 tubes (Greiner Bio-one, Monroe, NC) via retro-orbital bleeding. 5 μL of blood samples were mixed with 1 mL Natt-Herrick's stain (Eng Scientific Inc., NJ) and incubated for 5 min at room temperature. 20 μL of the sample was dispensed into the hemacytometer counting chamber and the dark blue stained white blood cells were counted.

The primary and metastatic tumor nodules, liver, spleen and pancreas were collected from the tumor bearing animals post-euthanasia, embedded in frozen section medium (Richard-Allan Neg 50, Thermo Scientific, Waltham, MA), flash frozen in liquid nitrogen and stored at −80 °C until used. The embedded tissues were cryo-sectioned into 10 μm thick sections using Microm HM550 cryostat (MICROM International GmbH, Germany). The section were mounted on to glass slides (SuperFrost Plus, Thermo Scientific, Waltham, MA), air dried at room temperature and fixed in 10% formalin for 10 min. Fixed sections were washed three times with PBS followed by water, stained in hematoxylin for 8 min rinsed in

water for 5 min and incubated in 1% acid alcohol for 30 s (clearing agent). Sections were rinsed and incubated in ammonia solution (bluing agent) for 30 s, rinsing in 95% alcohol, stained in eosin Y for 30 s, washed in 95% followed by 100% ethanol and finally by xylene substitute. The tissue samples were mounted with Fluoromount-G (Southern Biotech, AL), covered by a glass cover slip, and imaged with an Olympus BX61 fluorecence microscope.

In Vivo Drug Administration and Dosing Schedule

The orthotopic tumor bearing SCID beige mice were randomized into different treatment groups (n=6) and were administered with 4 weekly doses of gemcitabine (5 mg/kg) in PBS or loaded in gelatin nanoparticles suspended in PBS. The drug was administered to the animals intravenously via tail vein injections at day 0, 7, 14 and 21 and the animals were sacrificed by CO_2 inhalation followed by cervical dislocation after 28 days since the initiation of therapy. Tumor bearing animals dosed with PBS served as the control for the efficacy study of gemcitabine treatment. The animals were imaged by IVIS weekly during the course of therapy to monitor the tumor volume change as a function of luciferase activity.

Data Analysis and Statistics

Results were expressed as mean ± SD of the at least three independent experiments. Data was analyzed by Student's t-test. Differences were considered statistically significant at $p<0.05$.

RESULTS

Synthesis and Characterization of Gem-SPDP Conjugate

The illustration in Figure 1 shows the synthesis scheme of Gem-SPDP conjugate and subsequent conjugation with thiolated type B gelatin to form Gem-Gel conjugate. The TLC analysis of the reaction showed 3 distinct bands corresponding to unreacted gemcitabine, Gem-SPDP and unreacted SPDP (Figure 2A, lane 1). The separation of the product through normal phase flash chromatography yielded unreacted SPDP (Lane 2) and the Gem-SPDP conjugate (Lane 3) with an Rf value of 0.67. Lane 4 corresponds to the intermediate fraction between elution fractions of SPDP and conjugate, showing a faint band for SPDP alone with no signature for the presence of Gem-SPDP conjugate indicating that we could efficiently extract the pure conjugate without interference from the unreacted SPDP.

An HPLC method was developed to study the retention time of SPDP, Gem and Gem-SPDP and confirm the purity of the column purified Gem-SPDP conjugate (Figure 2 B–D). SPDP showed a retention time of 1.940 min while Gem-SPDP showed a similar retention time of 2.05 min as opposed to Gemcitabine alone, which eluted at 3.54 min. Most importantly, the purified conjugate did not show any peak corresponding to free gemcitabine, confirming successful removal of unreacted gemcitabine from the reaction product. The Gem-SPDP conjugate was further subjected to a treatment with 5 mM DTT to disrupt the disulfide linkage and release thiolated gemcitabine drug, which had a peak at around 3.6 min, similar to gemcitabine (Figure 2E). The total yield of the Gem-SPDP conjugate could also be calculated against a standard curve of gemcitabine and was found to be 42.2% (w/w).

The purified Gem-SPDP conjugate was also characterized by ^{1}H NMR spectroscopy to confirm the conjugation and monitor product purity. The NMR spectra from SPDP showed the signature peaks including the aromatic protons between 6–7 (Figure 3A, red box), while the spectra from gemcitabine did not show any peaks in that region except the amine protons around 7.9 ppm (Figure 3B, blue box). Another key peak in the spectra from SPDP is from the proton in the succinimide ring (around 2.6 ppm). Interestingly, the NMR spectra of the Gem-SPDP conjugate showed a disappearance of peak corresponding to succinimide proton from SPDP and amine protons from Gem (Figure 3C, purple and blue arrow respectively), which suggests successful Gem-SPDP conjugation. We could also see a strong peak at 5.7 ppm corresponding to proton from dichloromethane (Figure 3C, green box), indicating the presence of residual solvent that was removed by overnight desiccation under vacuum. Finally, the identity of the Gem-SPDP conjugate was conclusively validated by LC-MS analysis. The elution peak at 2 min on the column showed a major peak at 461.1 in the MS spectra operating in positive ionization mode, which corresponds to the m+1 molecular weight of the conjugate. Additionally, weaker peaks were obtained at 462.1 and 463.1, which were attributed to the isotopic variants of the conjugate. The peak at 483.1 could be assigned to the sodium adduct of the conjugate.

Synthesis and Characterization of Control and Targeted Nanoparticles

Prior to its use for formulation, type B gelatin was treated for removal of endotoxin; the final treated product showed an endotoxin level of 0.08 EU/mg, which could be considered to be an endotoxin free product. The thiolation of the gelatin backbone was monitored by Ellman's reagent, which confirmed to be 23.5 ± 2.6 mM sulfahydryl group equivalent per gram of gelatin. Thiolated gelatin was reacted with purified Gem-SPDP to facilitate the Gem-Gel conjugation through disulfide bond (Figure 1). Gem-SPDP-Gel conjugate and Gem-Gel nanoparticles were subjected to DTT (to break disulfide linkage) and protease digestion (to cleave amide bond) prior to drug analysis by HPLC. Thiolated gelatin was also subjected to DTT alone, protease alone and DTT/protease combination to study the retention time of various products. HPLC retention time of all the products (Figure 4 A, B & C) show no interfering peak around 3.5 min, where the characteristic peak for gemcitabine is observed (Figure 2C). Compared to thiolated gelatin, only Gem-Gel nanoparticles released a product with retention time around 3.55 min with DTT, protease or DTT/protease combination treatment (Figure 4 D, E and F; blue arrow), which correlates with the retention time of free gemcitabine and confirms that disruption of disulfide linkage indeed is able to release the thiolated gemcitabine with retention time similar to free gemcitabine. Among all the treatment conditions to study gemcitabine release, treatment with both 0.2 mg/ml protease and 5 mM DTT released the highest amount of gemcitabine (Figure 4F), which simulated the intracellular environment of cancer cells (27). Based on the standard curve of gemcitabine, loading of drug in Gem-Gel conjugate could be calculated as 24.9% (w/w). This study shows that Gem-Gel nanoparticles could release the drug efficiently under the reducing conditions that mimic the tumor microenvironment. The Gem-Gel nanoparticles were used for further synthesis of PEG modified non-targeted and EGFR-targeted gelatin nanoparticles.

The average size and surface charge of the nanoparticles with different surface modification were measured with a Zetasizer. The mean particle diameters of different nanoparticles ranged between 150–250 nm, with an increase in the particle size on PEG and subsequent EGFR peptide modification (Table 1; Figure SI. 4). Zeta potential of different nanoparticles were in the range of -20 to -27, similar to thiolated blank gelatin nanoparticles. The size estimation from TEM images was done over 50 nanoparticles for both the samples (Figure 5). The size and surface charge properties of the different gelatin nanoparticle formulations were consistent with those obtained for the previous *in vitro* and *in vivo* studies (20–22).

Gemcitabine Cytotoxicity in Panc-1 Cells

The gemcitabine conjugate and the formulated unmodified, PEG-modified non-targeted, and EGFR-targeted drug loaded nanoparticles were tested for their cytotoxicity profile in Panc-1 pancreatic adenocarcinoma cells. Table 2 shows the IC_{50} values obtained for the various treatment groups, where the conjugate itself as well as the drug-loaded gelatin nanoparticles exhibit a superior cell killing efficiency compared to the free drug in solution. Among the treatment groups, Gem-SPDP appears to have the lowest IC_{50} value (8.39 ± 1.79 μM), which could be attributed to the well known high binding affinity of the succinimidyl group to the cell surface proteins that would result in their rapid uptake inside the cells (28). However, the Gem-SPDP conjugate would not serve as a viable therapeutic option *in vivo* and in clinic since it can non-specifically interact and bind to any protein in the body. Among the gelatin nanoparticle treatment groups, EGFRtargeted nanoparticles showed the lowest IC_{50} value of 17.08 ± 2.32 μM.

Orthotopic Pancreatic Tumor Model Development

We developed a surgical orthotopic pancreatic cancer model and studied the tumor growth and metastasis in nude as well as SCID beige mice. Nude mice showed a slower growth rate of the tumor with peak intensity at 7 weeks since the implantation of the cells (Supporting info SI 8A). The localized tumor growth was observed during the initial phase and imaging in ventral presentation of the mice did not show any metastatic site. The peak signal intensity was observed around 7 weeks after the surgery and the signal intensity thereafter started to decline probably due to metastasis associated signal dispersion (Supporting info SI 8C). In comparison, the tumor growth rate in SCID beige mice was far more rapid where the highest intensity was achieved in 4 weeks following which there was rapid accumulation of ascites fluid (Figure 5A). We also observed a drop in the total signal intensity primarily due to the dilution of the luciferin substrate, due to accumulation of the ascites. The orthotopic cancer model in SCID beige mice was selected for further evaluation and efficacy studies since the tumor growth was established in shorter time with rapid onset on metastasis (Supporting info SI 8B).

The increase in tumor burden led to an increased population of white blood cells in orthotopic tumor bearing mice (tumor size ~ 1,500 mm^3) compared to that of naïve animal ($p < 0.01$) and that from a subcutaneous tumor-bearing mouse (tumor size ~ 1000 mm^3), primarily due to higher tumor volume (Figure 6B). The tumor bearing SCID mice were dissected after 4 weeks post-surgery and the peritoneal cavity showed multiples metastatic tumor nodules along with the primary tumor at the site of injection (Figure 6C).

Splenomegaly was observed in the tumor bearing mice (length 2.4 cm; weight 0.303 g) as compared to spleen from a naïve mouse (length 1.7 cm; weight 0.117 g) that did not show any abnormal growth, suggesting that the circulating cancer cells infiltrate into the spleen (Supporting info, Fig SI 9). The histopathological analysis of hematoxylin and eosin (H&E) stained tumor tissue section at the primary site of injection showed dark stained center with cancer cells while the peripheral tissues showed staining pattern similar to the normal pancreatic tissue (Figure 7 A, B). This observation suggests that the tumor growth occurs at the confined site of injection and did not form any dispersed loci in the pancreas. The hematoxylin and eosin (H&E)-stained sections of the metastatic tumors from mesentery and peritoneum also showed cancerous tissues surrounded by normal tissues while the section of liver and spleen did not show any sign of neoplastic cells (Figure 7).

Anti-tumor Efficacy Studies

The established orthotopic pancreatic cancer model in SCID beige mice was used for studying the therapeutic potential of gemcitabine encapsulated in non-targeted and EGFR-targeted gelatin nanoparticles and its therapeutic effect was compared to untreated control and animals treated with gemcitabine in solution. The average intensity flux of the animals was calculated by IVIS imaging and the animals were randomized into four treatment groups, which received PBS or gemcitabine formulation (5 mg/kg) via tail vein injection every week for four weeks (Supporting information, Figure SI 10). During the course of therapy, animals were imaged by IVIS imaging to calculate the bioluminescence activity of Panc-1luc cells as a measure of tumor volume. The animals from the control group, injected with PBS only, showed a steady increase in the bioluminescence intensity, suggesting an increase in the total tumor volume. The animals treated with gemcitabine solution in PBS showed a minor improvement in prevention of tumor growth (14.5 % reduction in tumor growth) with no significant increase in therapeutic benefit compared to the control (Figure 8 A, B, E). This result is consistent with our previous observation, where subcutaneous pancreatic tumor bearing mice treated with gemcitabine in solution showed a marginal therapeutic benefit compared to the control (22). Among the groups of animals treated with gemcitabine encapsulated in gelatin nanoparticles, the EGFR-targeted nanoparticles showed an enhanced anti-tumor activity with a 68% reduction in tumor growth on day 28 (Figure 8 D, E). The animals treated with gemcitabine encapsulated in non-targeted gelatin nanoparticles showed a 50.3% reduction in tumor growth compared to the control (Figure 8 C, E). Thus, the efficacy study clearly demonstrates a superior anti-tumor activity from gemcitabine encapsulated in EGFR-targeted gelatin nanoparticles, which corroborates with our previous results in subcutaneous pancreatic cancer animal model (22). Most importantly, the gelatin nanoparticles retain their therapeutic advantage in the aggressive orthotopic pancreatic cancer model, which more closely recapitulates the actual disease. Histo-pathological evaluation of excised liver and spleen tissues from mice treated with non-targeted and EGFR-targeted nanoparticles also confirm that though these nanoparticles infiltrate into these tissues (21), they do not elicit any harmful effect to the organs as shown in the Supplemental (SI) Figure 11. Therefore, the EGFR-targeting strategy clearly shows a distinct merit over non-targeted approach in realizing a viable therapeutic approach with higher chances for success towards the treatment of pancreatic cancer.

DISCUSSION

The redox-responsive, control and EGFR-targeted type-B gelatin nanoparticles were formulated and characterized for therapy in pancreatic cancer cells. Gelatin is a biodegradable, biocompatible and non-immunogenic *GRAS* material that has been previously used extensively as a non-condensing natural polymer system for delivery of nucleic acids to the cells and *in vivo*. We extended the application of this delivery platform to a small cytotoxic drug and tested its potential as delivery vector for targeting pancreatic cancer in an aggressive orthotopic surgical model. The targeted gemcitabine-loaded nanoparticles have release of drug under reducing conditions, which validates that simulating the tumor microenvironment leads to the best release conditions, where ~90% of the drug is released within the first 6 hours (22). Targeted nanoparticles also show a cytotoxic effect on the cancer cells *in vitro*. The marginal improvement in the *in vitro* cytotoxicity profile of targeted nanoparticles compared to the non-PEG modified and non-targeted nanoparticles is largely due to normalized uptake of the particles by the cells over an extended period of incubation. Our previous time-dependent uptake study with different gelatin nanoparticles in Panc-1 cells demonstrated that the EGFR-targeted nanoparticles could enter the cells faster due to receptor-mediated endocytosis but difference is normalized over longer incubation periods (20). However, targeted nanoparticles have a favorable therapeutic benefit *in vivo*, primarily due to the EPR effect bestowed by the presence of PEG and targeting effect due to the presence of the peptide (21, 22). We have previously confirmed the biodistribution and efficacy of gelatin nanoparticles for combination treatment in pancreatic subcutaneous xenograft tumor model and our results indicated a superior pharmacokinetics and pharmacodynamic profile of the targeted nanoparticles and increased antitumor activity.

Pancreatic cancer tumor displays a highly heterogeneous composition with strong stromal content and complex interplay between different types of cells, cytokines, chemokines and extracellular matrix components. Majority of promising therapeutic approaches at the preclinical research level fail to succeed at the clinical stage primarily due to the lack of appropriate animal model with suitable manifestation of actual pancreatic tumor. In order to assess the suitability of the delivery platform in a clinically more relevant model, the therapeutic potential of these EGFR-targeted nanoparticles was tested in a well-characterized orthotopic pancreatic adenocarcinoma model in SCID beige mouse. The efficacy study confirms that the targeted nanoparticles outperform non-targeted nanoparticles and gemcitabine drug in solution with an efficient anti-tumor activity. Taken together, gelatin nanoparticles make an attractive delivery platform, amenable to chemical manipulations and optimization as well as capable of hosting the desired therapeutic molecule and ferrying it to the tumor.

Supplementary Material

Refer to Web version on PubMed Central for supplementary material.

ACKNOWLEDGEMENTS

We gratefully acknowledge Dr. Ganesh Thakur and Mr. Abhijit Kulkarni for assistance with flash-chromatography purification and LC/MS studies.

Funding Sources: This study was supported by the National Cancer Institute's Alliance in Nanotechnology for Cancer's Center for Cancer Nanotechnology Excellence (CCNE) grant U54-CA151881.

REFERENCES

1. Ko AH. Progress in the Treatment of Metastatic Pancreatic Cancer and the Search for Next Opportunities. Journal of clinical oncology : official journal of the American Society of Clinical Oncology. 2015 Jun 1; 33(16):1779–1786. PubMed PMID: 25918299. [PubMed: 25918299]
2. Li HY, Cui ZM, Chen J, Guo XZ, Li YY. Pancreatic cancer: diagnosis and treatments. Tumour biology : the journal of the International Society for Oncodevelopmental Biology and Medicine. 2015 Mar; 36(3):1375–1384. PubMed PMID: 25680410. [PubMed: 25680410]
3. Lowery MA, O'Reilly EM. Novel Therapeutics for Pancreatic Adenocarcinoma. Hematology/oncology clinics of North America. 2015 Aug; 29(4):777–787. PubMed PMID: 26226910. [PubMed: 26226910]
4. Bria E, Milella M, Gelibter A, Cuppone F, Pino MS, Ruggeri EM, et al. Gemcitabine-based combinations for inoperable pancreatic cancer: have we made real progress? A meta-analysis of 20 phase 3 trials. Cancer. 2007 Aug 1; 110(3):525–533. PubMed PMID: 17577216. [PubMed: 17577216]
5. Pollom EL, Koong AC, Ko AH. Treatment Approaches to Locally Advanced Pancreatic Adenocarcinoma. Hematology/oncology clinics of North America. 2015 Aug; 29(4):741–759. PubMed PMID: 26226908. [PubMed: 26226908]
6. Rubinson DA, Wolpin BM. Therapeutic Approaches for Metastatic Pancreatic Adenocarcinoma. Hematology/oncology clinics of North America. 2015 Aug; 29(4):761–776. PubMed PMID: 26226909. [PubMed: 26226909]
7. Seicean A, Petrusel L, Seicean R. New targeted therapies in pancreatic cancer. World journal of gastroenterology : WJG. 2015 May 28; 21(20):6127–6145. PubMed PMID: 26034349. Pubmed Central PMCID: 4445091. [PubMed: 26034349]
8. Sirohi B, Singh A, Dawood S, Shrikhande SV. Advances in chemotherapy for pancreatic cancer. Indian journal of surgical oncology. 2015; 6(1):47–56. PubMed PMID: 25937764. Pubmed Central PMCID: 4412866. [PubMed: 25937764]
9. Neesse A, Michl P, Frese KK, Feig C, Cook N, Jacobetz MA, et al. Stromal biology and therapy in pancreatic cancer. Gut. 2011 Jun; 60(6):861–868. PubMed PMID: 20966025. [PubMed: 20966025]
10. Wachtel MS, Xu KT, Zhang Y, Chiriva-Internati M, Frezza EE. Pancreas cancer survival in the gemcitabine era. Clinical medicine Oncology. 2008; 2:405–413. PubMed PMID: 21892307. Pubmed Central PMCID: 3161658. [PubMed: 21892307]
11. Olive KP, Jacobetz MA, Davidson CJ, Gopinathan A, McIntyre D, Honess D, et al. Inhibition of Hedgehog signaling enhances delivery of chemotherapy in a mouse model of pancreatic cancer. Science. 2009 Jun 12; 324(5933):1457–1461. PubMed PMID: 19460966. Pubmed Central PMCID: 2998180. [PubMed: 19460966]
12. Gillen S, Schuster T, Meyer Zum Buschenfelde C, Friess H, Kleeff J. Preoperative/neoadjuvant therapy in pancreatic cancer: a systematic review and meta-analysis of response and resection percentages. PLoS medicine. 2010 Apr.7(4):e1000267. PubMed PMID: 20422030. Pubmed Central PMCID: 2857873. [PubMed: 20422030]
13. Conroy T, Desseigne F, Ychou M, Bouche O, Guimbaud R, Becouarn Y, et al. FOLFIRINOX versus gemcitabine for metastatic pancreatic cancer. The New England journal of medicine. 2011 May 12; 364(19):1817–1825. PubMed PMID: 21561347. [PubMed: 21561347]
14. Kundranda MN, Niu J. Albumin-bound paclitaxel in solid tumors: clinical development and future directions. Drug design, development and therapy. 2015; 9:3767–377. PubMed PMID: 26244011. Pubmed Central PMCID: 4521678.

15. Kommareddy S, Amiji M. Preparation and evaluation of thiol-modified gelatin nanoparticles for intracellular DNA delivery in response to glutathione. Bioconjugate chemistry. 2005; 16(6):1423–1432. PubMed PMID: 16287238. [PubMed: 16287238]
16. Kommareddy S, Amiji M. Poly(ethylene glycol)-modified thiolated gelatin nanoparticles for glutathione-responsive intracellular DNA delivery. Nanomedicine : nanotechnology, biology, and medicine. 2007 Mar; 3(1):32–42. PubMed PMID: 17379167. Pubmed Central PMCID: 1885230.
17. Kommareddy S, Amiji M. Biodistribution and pharmacokinetic analysis of long-circulating thiolated gelatin nanoparticles following systemic administration in breast cancer-bearing mice. Journal of pharmaceutical sciences. 2007 Feb; 96(2):397–407. PubMed PMID: 17075865. [PubMed: 17075865]
18. Kommareddy S, Amiji MM. Cell Transfection and Analysis Using DNA-Loaded Gelatin Nanoparticles. CSH protocols. 2008; 2008 pdb prot4887. PubMed PMID: 21356669.
19. Kommareddy S, Amiji MM. Preparation and loading of gelatin nanoparticles. CSH protocols. 2008; 2008 pdb prot4885. PubMed PMID: 21356667.
20. Xu J, Amiji M. Therapeutic gene delivery and transfection in human pancreatic cancer cells using epidermal growth factor receptor-targeted gelatin nanoparticles. Journal of visualized experiments : JoVE. 2012; (59):e3612. PubMed PMID: 22231028. Pubmed Central PMCID: 3400379. [PubMed: 22231028]
21. Xu J, Gattacceca F, Amiji M. Biodistribution and pharmacokinetics of EGFR-targeted thiolated gelatin nanoparticles following systemic administration in pancreatic tumor-bearing mice. Molecular pharmaceutics. 2013 May 6; 10(5):2031–2044. PubMed PMID: 23544877. Pubmed Central PMCID: 3651790. [PubMed: 23544877]
22. Xu J, Singh A, Amiji MM. Redox-responsive targeted gelatin nanoparticles for delivery of combination wt-p53 expressing plasmid DNA and gemcitabine in the treatment of pancreatic cancer. BMC cancer. 2014; 14:75. PubMed PMID: 24507760. Pubmed Central PMCID: 3927583. [PubMed: 24507760]
23. Mazur PK, Siveke JT. Genetically engineered mouse models of pancreatic cancer: unravelling tumour biology and progressing translational oncology. Gut. 2012 Oct; 61(10):1488–1500. PubMed PMID: 21873467. [PubMed: 21873467]
24. Kim MP, Evans DB, Wang H, Abbruzzese JL, Fleming JB, Gallick GE. Generation of orthotopic and heterotopic human pancreatic cancer xenografts in immunodeficient mice. Nature protocols. 2009; 4(11):1670–1680. PubMed PMID: 19876027. Pubmed Central PMCID: 4203372. [PubMed: 19876027]
25. Schutte U, Bisht S, Brossart P, Feldmann G. Recent developments of transgenic and xenograft mouse models of pancreatic cancer for translational research. Expert opinion on drug discovery. 2011 Jan; 6(1):33–48. PubMed PMID: 22646825. [PubMed: 22646825]
26. Drake JM, Gabriel CL, Henry MD. Assessing tumor growth and distribution in a model of prostate cancer metastasis using bioluminescence imaging. Clinical & experimental metastasis. 2005; 22(8):674–684. PubMed PMID: 16703413. Epub 2006/05/17. eng. [PubMed: 16703413]
27. Navarro J, Obrador E, Carretero J, Petschen I, Avino J, Perez P, et al. Changes in glutathione status and the antioxidant system in blood and in cancer cells associate with tumour growth in vivo. Free radical biology & medicine. 1999 Feb; 26(3–4):410–418. PubMed PMID: 9895233. [PubMed: 9895233]
28. Quah BJ, Parish CR. The use of carboxyfluorescein diacetate succinimidyl ester (CFSE) to monitor lymphocyte proliferation. Journal of visualized experiments : JoVE. 2010; (44) PubMed PMID: 20972413. Pubmed Central PMCID: 3185625.

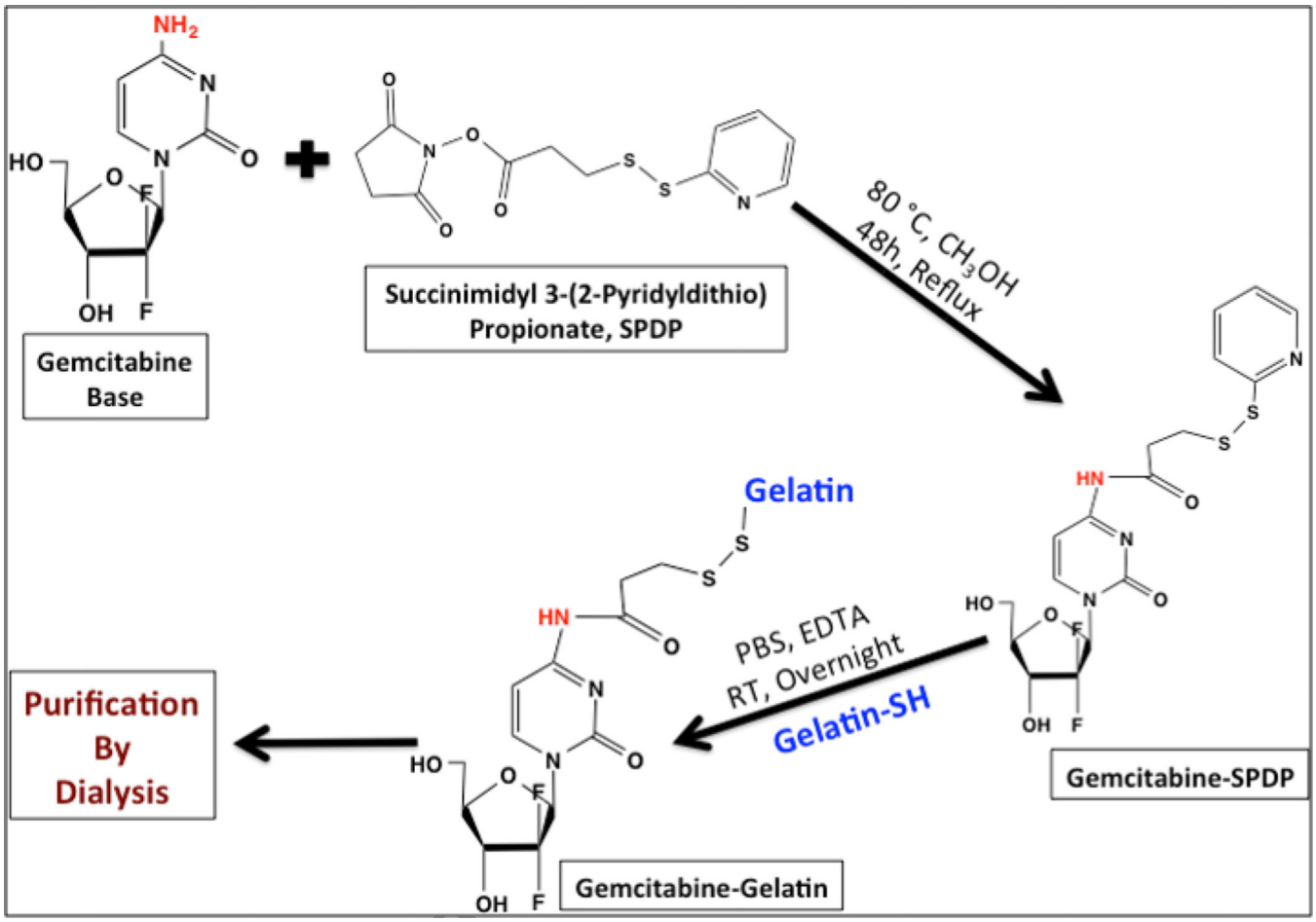

Figure 1.

Schematic representation for the chemical synthesis of gemcitabine-SPDP derivative (Gem-SPDP) and the disulfide conjugation of gemcitabine-SPDP with thiolated gelatin (Gem-Gel).

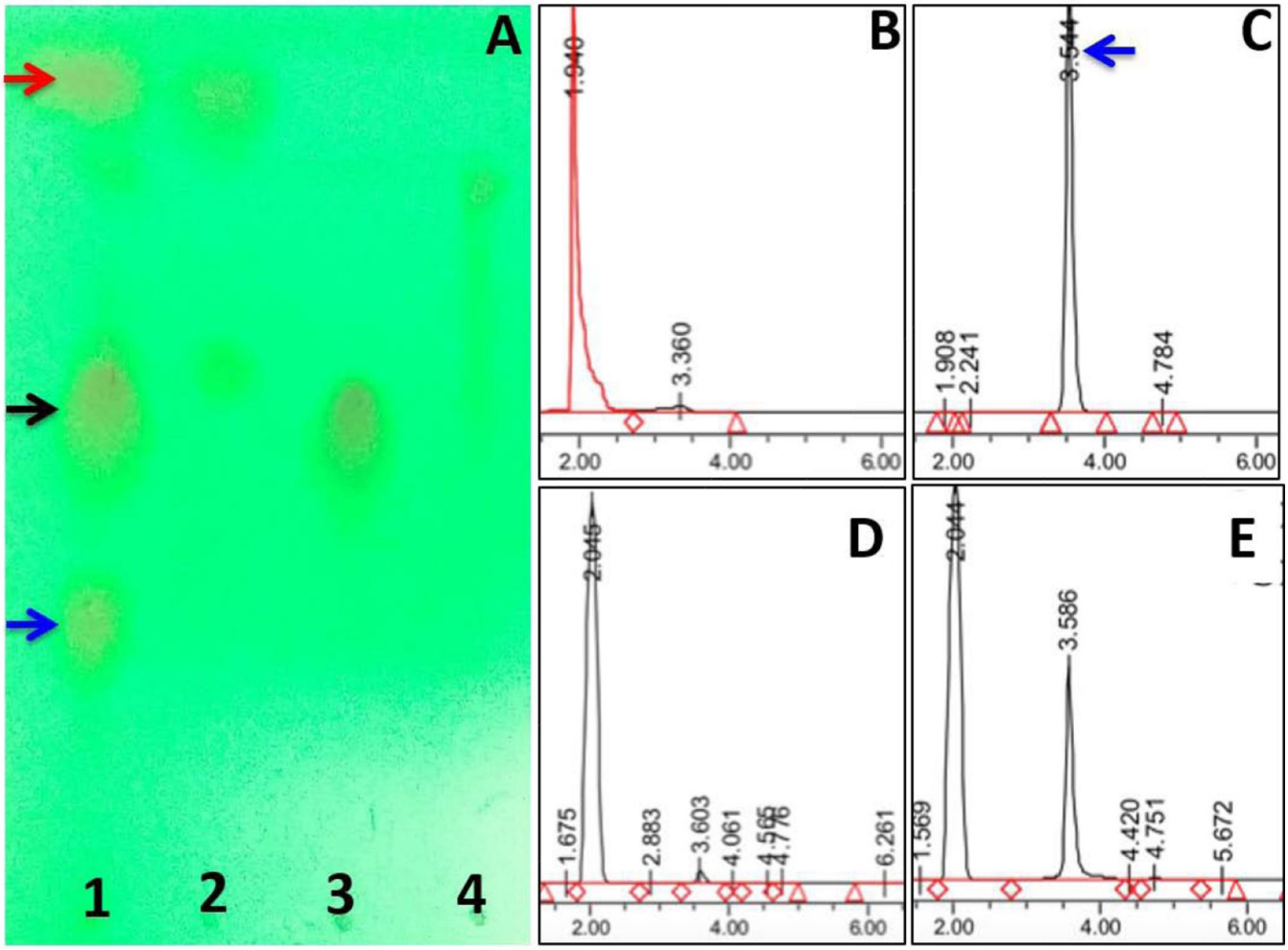

Figure 2.

Thin-layer chromatography image showing the bands corresponding to gemcitabine (blue arrow), SPDP (red arrow) and the gemcitabine-conjugated with SPDP (Gem-SPDP) (black arrow) in unpurified fraction (lane 1) and in purified fractions (lanes 2, 3 and 4) (A). The high performance liquid chromatography (HPLC) chromatograms showing the retention time of SPDP, gemcitabine base (Gem), Gem-SPDP conjugate and the conjugate treated with 5 mM dithiothreitol (DTT) (to disrupt the disulfide bonds), respectively (B,C,D,E). x-axis on each chromatogram represents elution time in min and y-axis shows relative peak intensities in arbitrary units (a.u.).

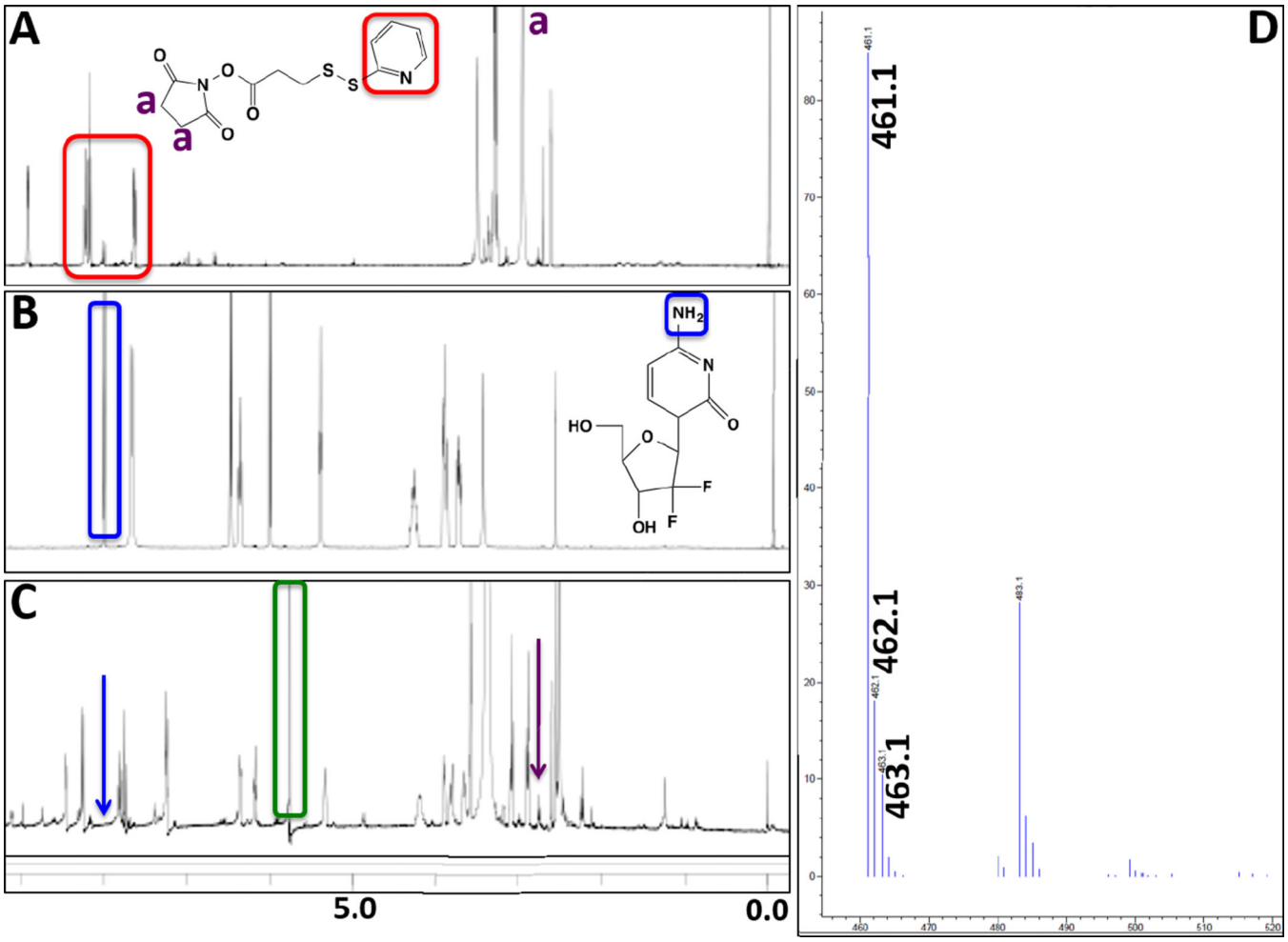

Figure 3.

^{1}H-NMR spectra of SPDP (A), gemcitabine base (Gem) (B), and gemcitabine-SPDP conjugate (Gem-SPDP) (C). The highlighted peaks correspond to the marked protons in the various derivatives. (D) Positive mode mass spectrometer spectra of the Gem-SPDP conjugate showing the peak m+1 peak at 461.1 and sodium adduct peak at 483.1 while the peaks at 462.1 and 463.1 correspond to isotope variants.

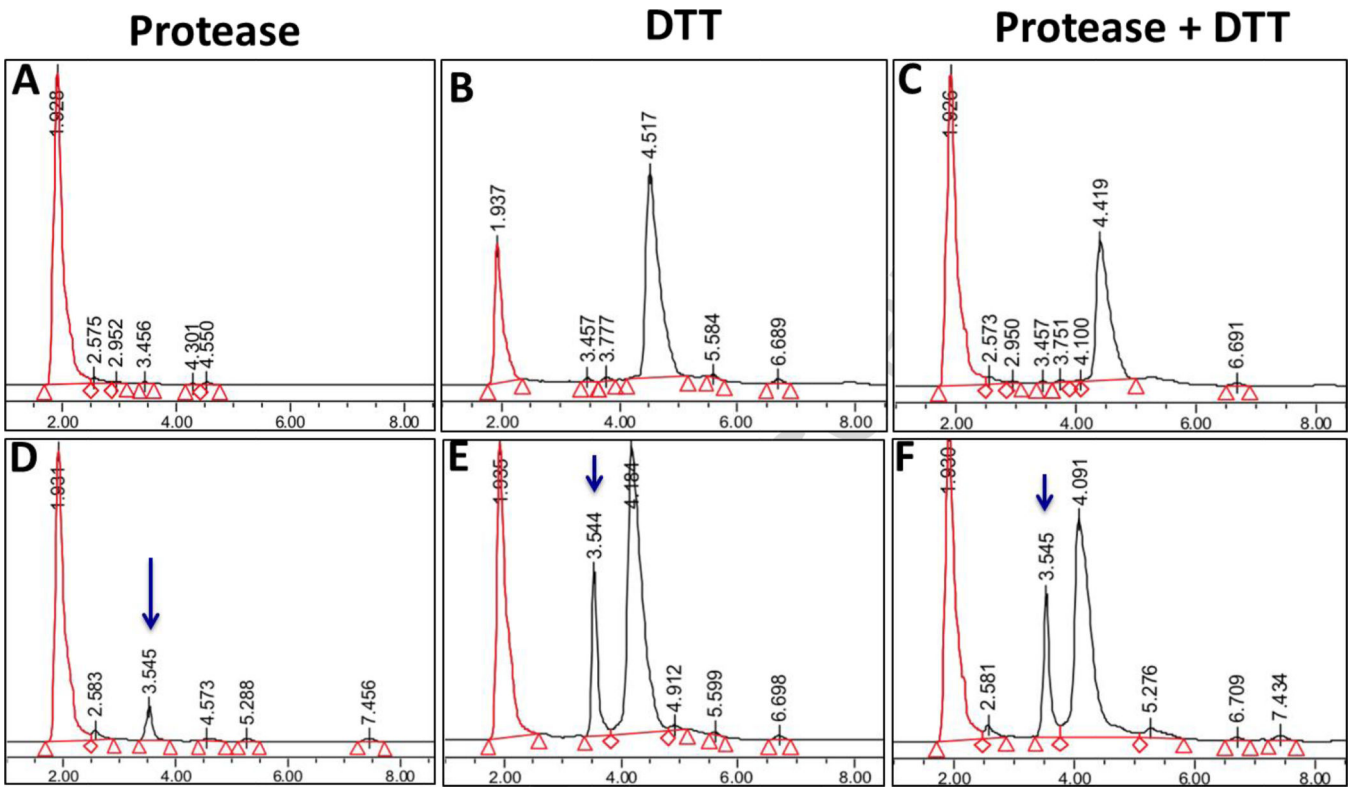

Figure 4.

High performance liquid chromatography (HPLC) chromatograms obtained from thiolated gelatin (Top Panel) and gemcitabine-conjugated thiolated gelatin (Gem-Gel) nanoparticles (Bottom Panel) following treatments with protease (A,D), with 5 mM dithiothreitol (B,E), and with combination protease and dithiothreitol (C,F). The x-axis on each chromatogram represents elution time in minutes and the y-axis shows relative peak intensities in arbitrary units (a.u.).

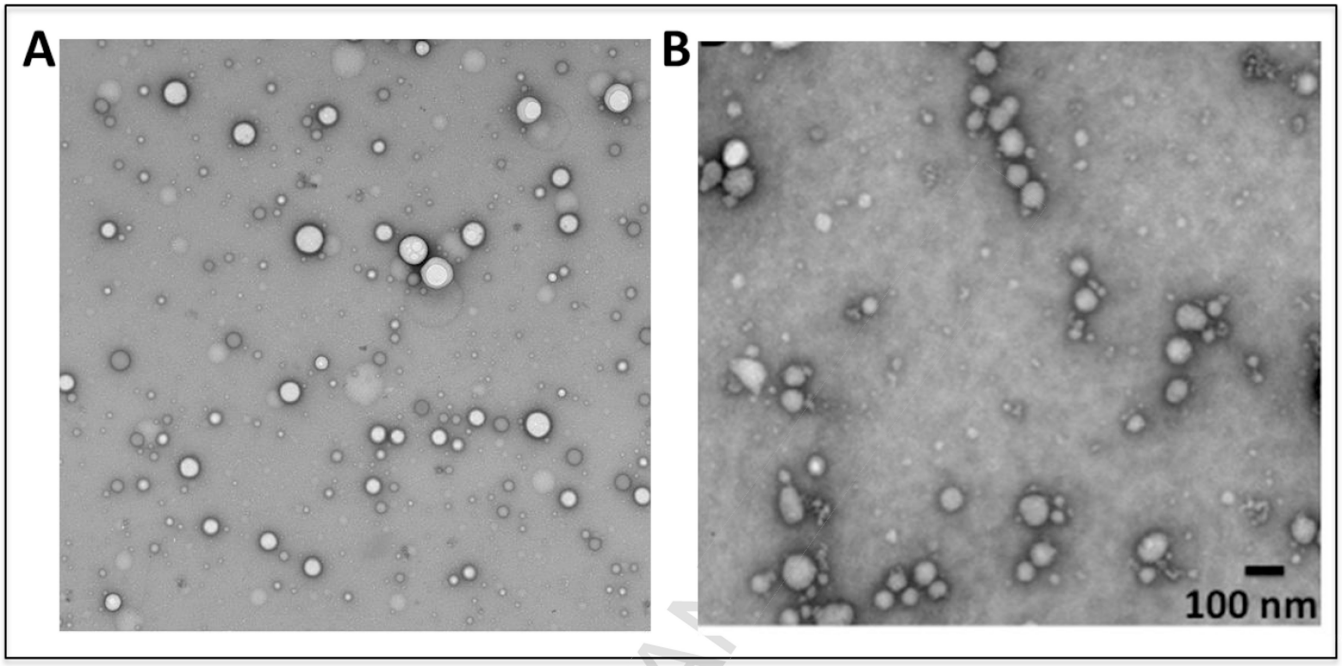

Figure 5.

Transmission electron microscopy (TEM) images of control (without gemcitabine) (A) and gemcitabine-encapsulated (B) type B gelatin nanoparticles. The nanoparticles show spherical morphology with size that matches the dynamic light scattering data. The samples were negatively stained with 1.5% uranyl acetate prior to imaging.

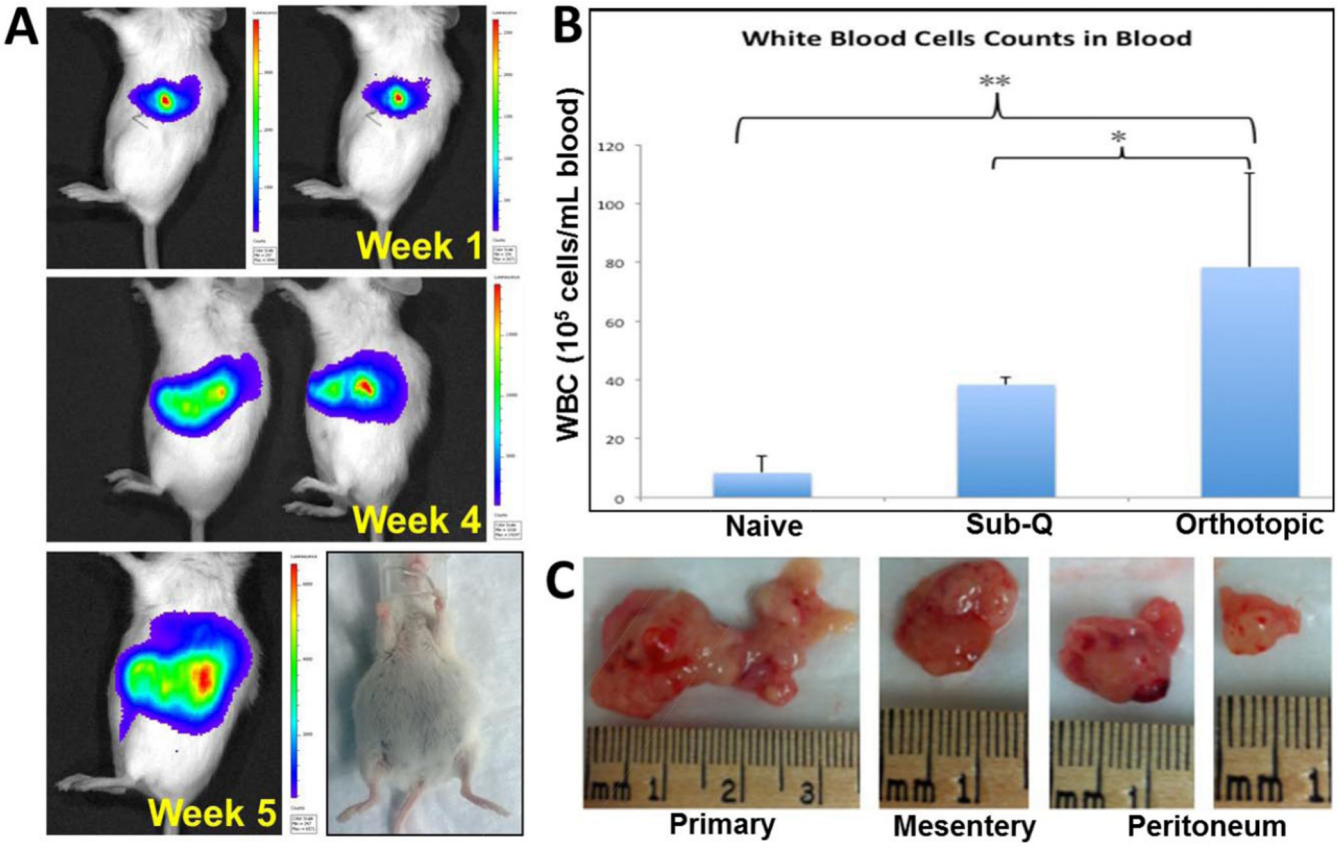

Figure 6.

Characterization of orthotopic pancreatic adenocarcinoma model in SCID beige mouse (A) Images showing the bioluminescence intensity obtained from IVIS imaging of mice injected with Panc-1 luc surgically in the pancreas with time post-surgery. All mice show accumulation of ascites fluid in their peritoneal cavity. (B) White blood cell count obtained from the blood of naïve, subcutaneous tumor and orthotopic tumor bearing mice, which is significantly higher for the tumor bearing animals; **($p < 0.01$); * ($p < 0.05$)). (C) Image of primary tumors excised from the site of injection and secondary tumor nodules excised from mesentery and peritoneum.

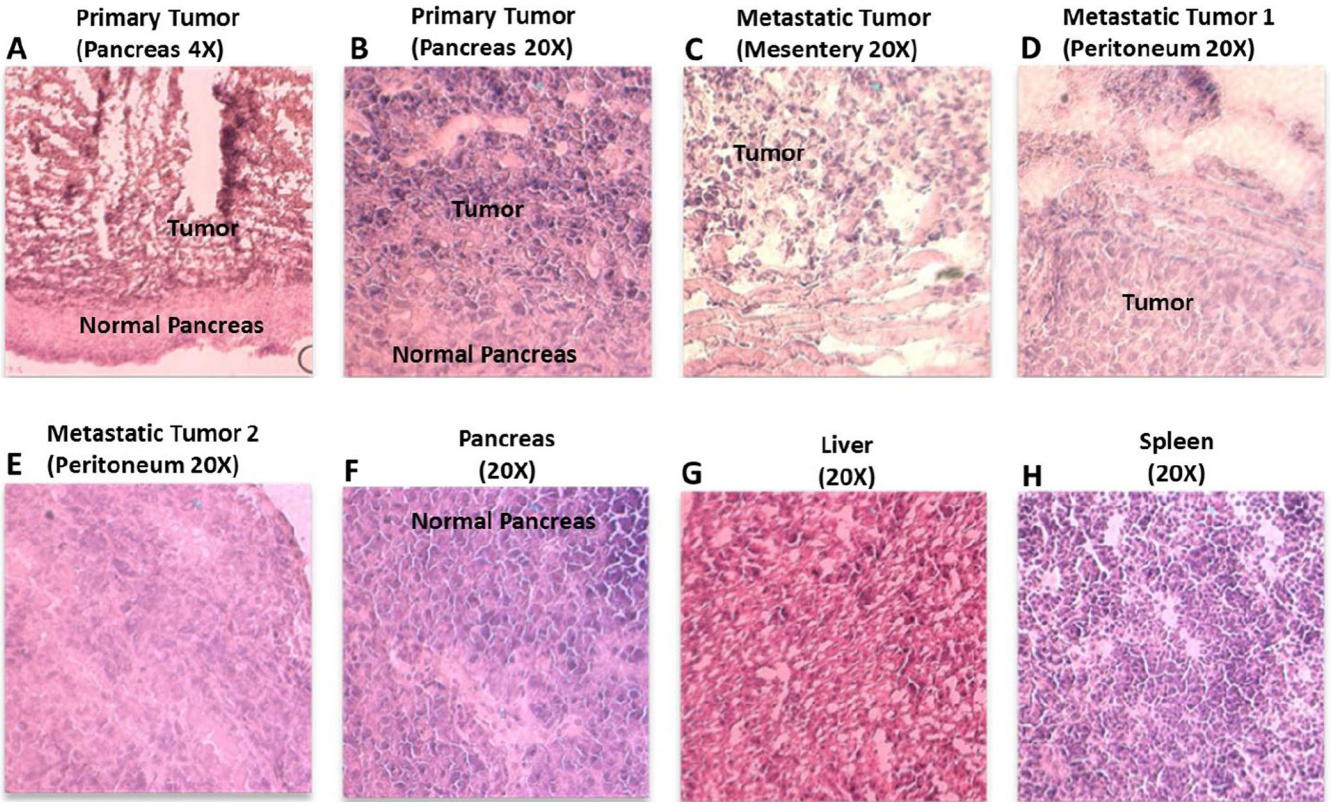

Figure 7.

Hematoxylin and eosin (H&E) stained imaging of tumor and tissue section of orthotopic pancreatic adenocarcinoma tumor bearing mice. The tumor from primary site of injection (A, B) and those resected from mesentery (C) and peritoneum (D, E) showed cancer cells surrounded with normal cells unlike a normal pancreas (F) while sections from liver (G) and spleen (H) did not show any metastatic sites or neoplastic cells.

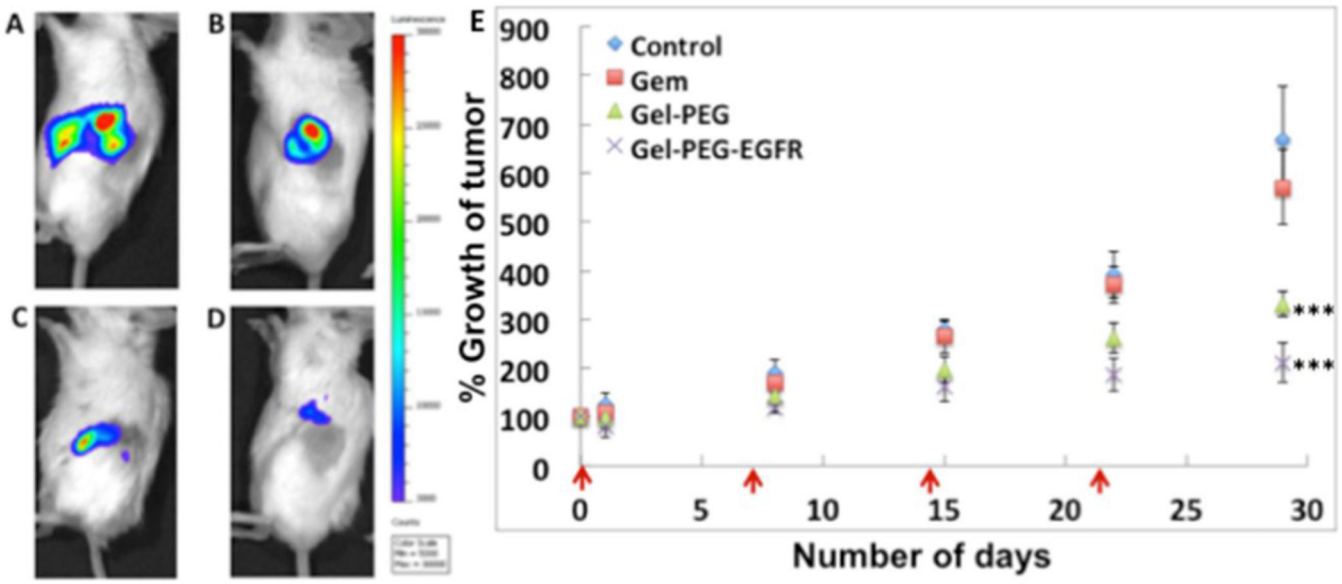

Figure 8.

Efficacy studies in orthotopic pancreatic adenocarcinoma bearing SCID beige mice. Representative IVIS images of mice treated with phosphate-buffered saline (PBS, pH 7.4) alone (A), gemcitabine solution in PBS (B), gemcitabine loaded non-targeted gelatin nanoparticles and gemcitabine loaded EGFR-targeted gelatin nanoparticles after 28 days of weekly treatment. The dosing scheme was intravenous via tail-vein injections and gemcitabine was administered to a dose of 5 mg/kg for 4 weeks, once a week in all of the formulations. The analysis of tumor growth shows that drug administered in gelatin nanoparticles show excellent anti-tumor activity (E) with EGFR-targeted nanoparticles showing a 68 % reduction in tumor growth profile.

Table 1

Table showing the particle diameter and surface charge (zeta potential) of the gemcitabine-conjugated gelatin (Gem-Gel), poly(ethylene glycol)-modified (PEG-Gem-Gel), and epidermal growth factor receptor targeted (EFGR-targeted Gem-Gel) nanoparticles.

Formulation	Particle Diameter ± SD (nm)	Zeta Potential ± SD (mV)
Gem-Gel	114.8 ± 11.5*	−27.1 ± 1.62
PEG-Gem-Gel	163.7 ± 40.2	−23.5 ± 3.93
EGFR-Gem-Gel	221.3 ± 32.4	−20.3 ± 2.25

*Mean ± S.D. (n = 3)

Table 2

The IC_{50} cytotoxicity assessment of gemcitabine base and gemcitabine in gelatin nanoparticles administered in Panc-1 human pancreatic adenocarcinoma cells.

Formulation	IC_{50} Value (μM)
Gemcitabine	123.9 ± 23.9*
SPDP	N/A
Gem-SPDP	8.39 ± 1.79
Gem-Gel Nanoparticles	24.76 ± 7.99
Gem-Gel-PEG	20.08 ± 6.97
Gem-Gel-PEG-EGFR	17.08 ± 2.32

*Mean ± S.D. (n = 3)